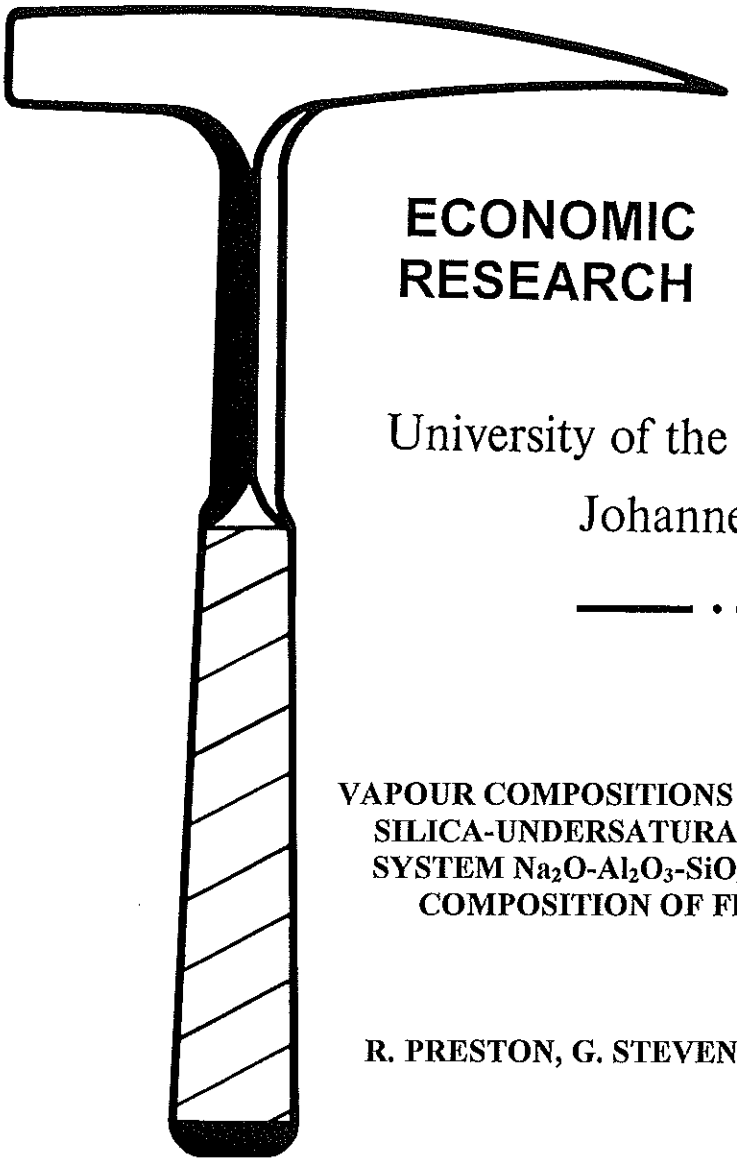

ECONOMIC GEOLOGY
RESEARCH INSTITUTE

University of the Witwatersrand
Johannesburg

VAPOUR COMPOSITIONS IN EQUILIBRIUM WITH SILICA-UNDERSATURATED MAGMAS IN THE SYSTEM Na_2O-Al_2O_3-SiO_2-H_2O: CLUES TO THE COMPOSITION OF FENITIZING FLUIDS

R. PRESTON, G. STEVENS and T. S. McCARTHY

INFORMATION CIRCULAR No. 340

UNIVERSITY OF THE WITWATERSRAND
JOHANNESBURG

VAPOUR COMPOSITIONS IN EQUILIBRIUM WITH SILICA-UNDERSATURATED MAGMAS IN THE SYSTEM Na_2O-Al_2O_3-SiO_2-H_2O: CLUES TO THE COMPOSITION OF FENITIZING FLUIDS

by

R. PRESTON[1], G. STEVENS[1] AND T. S. McCARTHY[2]

([1]Economic Geology Research Institute, University of the Witwatersrand, Private Bag 3, WITS 2050, South Africa, [2]Department of Geology, University of the Witwatersrand, Private Bag 3, WITS 2050, South Africa)

**ECONOMIC GEOLOGY RESEARCH INSTITUTE
INFORMATION CIRCULAR No.340**

January, 2000

VAPOUR COMPOSITIONS IN EQUILIBRIUM WITH SILICA-UNDERSATURATED MAGMAS IN THE SYSTEM Na_2O-Al_2O_3-SiO_2-H_2O: CLUES TO THE COMPOSITION OF FENITIZING FLUIDS

ABSTRACT

Fenites result from alkali metasomatism associated with silica-undersaturated alkaline magmatism, and are characterised by addition of alkalis, albitization, nephelinization, diffusion of silica and the formation of alkali pyroxenes and amphiboles. In an attempt to constrain the fluid compositions involved, we have investigated the compositions of aqueous fluid phases in equilibrium with various silica-undersaturated alkaline magmas within the chemical system Al_2O_3-Na_2O-SiO_2-H_2O at conditions of 850°C and 1 kilobar. Experiments were run for 120 hours in cold-seal pressure vessels, housing a platinum capsule containing an Al_2O_3-Na_2O-SiO_2 mixture and up to 50wt% deionised water. Starting compositions straddle the nepheline-albite join, and included peralkaline and alkali-granitoid compositions.

The quenched run products all contain a homogeneous glass and an aqueous fluid, and in most cases, a radial crystalline phase, which often occurs as spherical beads. These never occur as inclusions in the glass and are interpreted to be a fluid-quench phase. Several glasses also contain albite, nepheline or quartz crystals.

Starting compositions plotting on the peralkaline side of the nepheline-albite join, in Al_2O_3-Na_2O-SiO_2 space, produced aqueous fluids in equilibrium with melt that were highly enriched in dissolved solids (SiO_2, Al_2O_3 and Na_2O, in the range 40 - 55 wt%). Fluid compositions in crystal-free runs were calculated using a mass balance approach that incorporated the composition of the glass (determined by EMPA) and carefully determined masses of the run products and starting materials. A typical calculated fluid composition, produced in conjunction with a melt consisting of SiO_2 = 33.91, Al_2O_3 = 30.23 and Na_2O = 19.98 (all in wt%), is: 16 wt% SiO_2, 12 wt% Al_2O_3, 27 wt% Na_2O and 45 wt% H_2O.

Model calculations indicate that melt compositions near nepheline on the nepheline-albite join are in equilibrium with fluids that are capable of converting granite to nepheline-syenite composition at very low fluid/rock ratios. Albitization and dissolution of quartz (in the form of sodium metasilicate), formation of sodic pyriboles (acmite) and, ultimately, nepheline is characteristic of the process modelled in this study and is analogous to the features and processes observed in natural fenites. In addition, fenitization is accompanied by significant volume increase (up to 33%), which could be responsible for granulation textures commonly observed in fenite aureoles.

oOo

VAPOUR COMPOSITIONS IN EQUILIBRIUM WITH SILICA UNDERSATURATED MAGMAS IN THE SYSTEM Na_2O-Al_2O_3-SiO_2-H_2O: CLUES TO THE COMPOSITION OF FENITIZING FLUIDS

CONTENTS

oOo

Published by the Economic Geology Research Institute
Department of Geology
University of the Witwatersrand
1 Jan Smuts Avenue
Johannesburg 2001

ISBN 1-86838-267-2

VAPOUR COMPOSITIONS IN EQUILIBRIUM WITH SILICA-UNDERSATURATED MAGMAS IN THE SYSTEM Na_2O-Al_2O_3-SiO_2-H_2O: CLUES TO THE COMPOSITION OF FENITIZING FLUIDS

INTRODUCTION

Extensive alkali metasomatism is a common phenomenon around alkaline intrusions. Results from numerous studies published over the last eighty years on this metasomatism, termed fenitization, have documented the mineralogical and geochemical changes induced by the process. Reviews may be found in McKie (1966), Le Bas (1987) and Gittins (1989). Despite this good knowledge of the characteristics of fenitized rocks, the composition of the volatile phase that drives the process is far less well understood. Experimental studies represent one of the few means of directly measuring the composition of the fluids involved in fenitization, but owing to the technical difficulties associated with this approach, very little data exists. Typically, in experiments of this type, the sample volumes are extremely small, isochemical quenching of equilibrium run products is impossible and consequently, the fluid phase retrieved is not normally representative of the fluid which existed at high pressure and temperature. Despite these difficulties, an experimental approach may represent the best technique for quantifying the composition of fenitizing fluids, particularly so when it is considered that eighty years of study on natural rocks has failed to answer this specific question. Thus, the aims of this study are to investigate the equilibrium compositions of melts and fluids in the relevant portions of the simplified chemical system Na_2O-Al_2O_3-SiO_2-H_2O, and to use the derived fluid compositions to model the process of fenitization.

Fenites and Fenitization: Some Varied Definitions

Fenites were first described by Brögger (1921), in his pioneering work on the rocks of the Fen Complex in southern Norway. He defined a suite of rocks whose compositions were originally granitic and which were subsequently metasomatically altered towards an alkali-syenitic composition by solutions sourced from an ijolite-melteigite magma within the complex (McKie, 1966). The term "fenite" has since taken on a far more general connotation, and encompasses a wide spectrum of alteration products of variable composition within the immediate environs of silica-undersaturated, alkaline complexes. Together with other workers (e.g. Currie and Ferguson, 1971, Gittins, 1989), McKie (1966) stated that fenites are normally associated with alkaline igneous intrusions containing carbonatite, and manifest as an aureole of metasomatized rocks, grading outward from rocks indistinguishable from alkaline igneous varieties, implying that the development of fenites is intimately related to secondary processes operating within and around carbonatite complexes. According to Gittins (1989), fenitizing fluids are derived principally from carbonatite rather than ijolite or nephelinite magma.

Garson *et al.* (1984), together with Morogan and Woolley (1989), cited evidence that fenites develop in both carbonatite-absent and carbonatite-present situations. A study of the Alnö carbonatite complex in Sweden by Morogan and Woolley (1989) documented the development of fenites through two main types of fluid, which were related to two

different magmatic sources; carbonatitic and ijolitic. This implies that two important sources of fenitizing agent were active, with different characteristics reflecting the different compositions of the magma driving the alteration. A definition for fenitization proposed by Garson *et al.* (1984) expanded the meaning to include any Na-K-Fe metasomatic alteration, whether driven by an alkaline silicate or carbonatitc magma and irrespective of the chemistry of either the host rock or the fenitizing agent. The conclusions outlined in work by Rubie and Gunter (1983), on the role of speciation in alkaline igneous fluids during metasomatism, provided some clarification – fenitization produced around CO_2-poor, silica-undersaturated intrusions (i.e. ijolites and nephelinites), develops at high temperatures (> 700°C; Le Bas, 1987) in the presence of a CO_2 - poor fluid phase.

The process of fenitization is complicated by the fact that it is controlled by a number of different variables including: (1) the chemical composition of the magma driving the metasomatism; (2) the composition of the fluids emanating from the magma; (3) the depth of intrusion, and therefore ambient temperature of the country rock; (4) the chemical composition of the country rocks; and (5) the interaction of a meteoric water component (Le Bas, 1987). Despite the numerous investigations that have been carried out in the past, there remains considerable debate as to the detailed mechanism of the process of fenitization and the conditions under which it operates. The details of the process differ from locality to locality and examples proving both carbonatite-free and carbonatite-present fenitization may be stated. The process of fenitization is exemplified, in the most general case, by the introduction of Na, K, Ca, Mg and Fe (mainly Fe^{3+}) and loss of silica resulting in feldspathization and nephelinization and the formation of alkali pyroxenes and amphiboles (Dawson and Smith, 1992). Differences in the mineralogy of fenites appear to result from whichever alkali ion dominates in the fenitizing fluids at a given complex, resulting in the formation of either sodic or potassic fenites.

Mineralogical and Petrographic Characteristics

The mineralogical and petrographic characteristics of fenites have been well documented in the literature from many localities (e.g. McKie, 1966; Currie, 1971; Currie and Ferguson 1971, 1972; Cooper, 1971; Siemiatkowska and Martin, 1975; Vartiainen and Woolley, 1976; Rubie, 1982; Robins and Tysseland, 1983; Garson *et al.*, 1984; Robins, 1984; Kresten and Morogan, 1986; Morogan and Woolley, 1988; Currie *et al.*, 1992; Pearson and Taylor, 1996). Several different classification schemes for fenites have been proposed. Kresten (1988), after studying the Alnö Complex in Sweden, where differences in chemistry, mineralogy and petrography are noted between contact rocks and fenitized material within the metasomatic aureole, subdivided fenites into three main zones based on their spatial relationship to the alkali intrusion (Fig. 1):

(1) *contact fenites:* rocks developed in the immediate vicinity of the source of the fenitizing fluid. These rocks represent the highest grade of fenitization, and usually the highest temperature type. The mineralogical and petrographic characteristics of these fenites differ greatly from those observed in the aureole, and these rocks are regarded as the products of multiple phases of fenitization;

(2) *aureole fenites:* occupy considerably larger areas than contact fenites and can be subdivided petrographically, as described by Kresten (1987) (Fig. 2). Contacts between successive zones are most often gradational, unless primary or secondary heterogeneities are present in the host rock, and;
(3) *vein fenites:* result from fluid channeling along cracks, fracture zones and other structural heterogeneities, which may cause fenitization outside of the more continuous metasomatic aureole.

Kresten and Morogan (1986), in a study of fenitization at the Fen Complex, based their nomenclature for fenites upon the increasing grade of fenitization as reflected by microstructures and mineral parageneses. They identified :

(1) *low-grade fenites* (aureole fenites as described above) where the least stable minerals (i.e. quartz, K-feldspar and biotite), are preserved;
(2) *medium-grade fenites* (also aureole fenites) which preserve little of the original mineral paragenesis and where microstructures are indicative of replacement and recrystallization; and
(3) *high-grade fenites* comprising entirely newly formed mineral assemblages. Microstructural evidence points toward more complete and intense recrystallization.

The fundamental differences in the nature of fenites observed from various localities are dependent on a number of factors:

(1) the composition of the protolith material, that exerts a primary control on the final composition and mineral assemblage of the metasomatized material; and
(2) variations in the chemical and physical properties of the volatile phase, which are, in turn, related to the nature of the intruding magma and the degree of its evolution (Kresten and Morogan, 1986).

The process of fenitization generally includes feldspathization, nephelinization and the formation of alkali pyroxenes and amphiboles (depending on whether fenitization is sodic or potassic), with concomitant loss, or replacement of quartz (Dawson and Smith 1992).

Le Bas (1987) provided a summary of the development of fenites around both ijolite/nephelinite and carbonatite bodies. Fenites associated with ijolite intrusions are said to form via the ultimate fractionation of a nephelinite body towards one of ijolitic composition at high temperatures (> 700°C) reflected by the compositions of feldspars (commonly $Or_{40\text{-}60}Ab_{60\text{-}40}$) and sub-solidus texture of the fenites, whereas the compositions of alkali feldspar (almost pure albite: $Ab_{>90}$ or orthoclase: $Or_{>85}$) of fenites around carbonatites reflect much lower temperatures of fenitization (below 550°C). In the case of fenites associated with ijolitic magmas, mineralogical zonation (Fig. 3) is pronounced within the metasomatic aureole. Pyroxene grades from weakly sodic aegirine-augite near the aureole-country rock contact to almost pure aegirine in the aureole zone closest to the intrusion. Feldspar produced near the aureole-intrusion contact is usually hypersolvus alkali feldspar ($Or_{40\text{-}60}Ab_{60\text{-}40}$) and original sub-solvus feldspars of

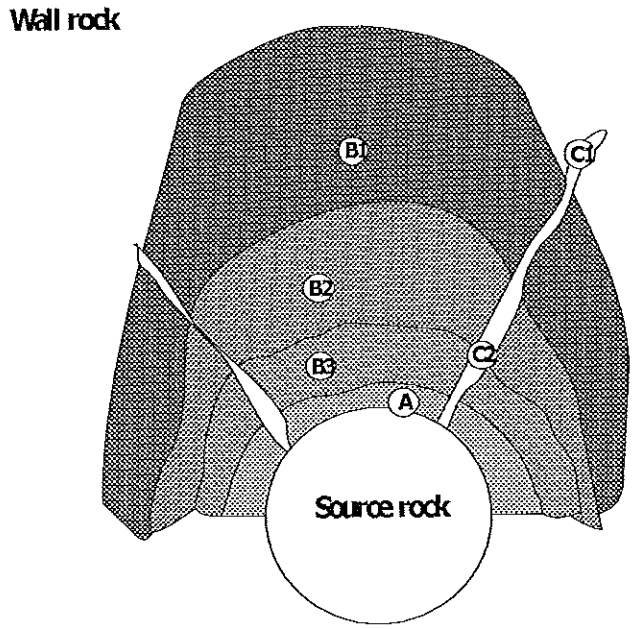

Figure 1: Schematic diagram showing the classification of fenites according to the geologic setting at Fen, Norway. Contact fenites (A) and aureole fenites (B3 = high grade; B2 = medium grade; B1 = low grade) show significant mineralogical and geochemical differences. Vein fenites are of local extent and develop around fractures, with subsequent fenitization superimposed on aureole fenites (C2) and unaltered wall rock (C1) (after Kresten, 1988).

the country rock survive in the outer zones. Aluminium is reported to remain relatively immobile during the process. Fenites produced around carbonatite intrusions seem to be more varied in character. Le Bas (1987) stated that fenitization in this case is almost exclusively developed in association with sövites, dolomitic carbonatites and rarely microsövites. Depth of emplacement, and therefore vertical temperature gradients, are important when considering fenitization associated with carbonatite. The uppermost parts of sövites are characterized by strongly potassic alteration along with the formation of pure K-feldspar lithologies ($Or_{>85}$). In older more deeply eroded examples, feldspathic fenites developed around sövites are albite rich ($Ab_{>90}$).

Chemistry of Fenitization: Mass Transfer and Volume-change Considerations

Detailed studies of the chemical changes that take place during fenitization began with the work by Von Eckermann (1948) and Strauss and Truter (1950). Later work on this subject includes that of Saether (1957), Verwoerd (1966), McKie (1966), Vartiainen and Woolley (1976), Appleyard and Woolley (1979), Rubie (1982), Kresten (1988) and Morogan (1984). Early techniques of calculating mass transfer and volume change during fenitization included the use of variation diagrams of cations vs. silica on the basis of 160 oxygens or 100 oxygens, and showed a general increase of most cations and a silica decrease during progressive fenitization. Mass transfer calculations using the standard cell of 100 anions method makes the fundamental assumption that the fenitization is

characterized by immobile oxygen, which approximates to constant-volume replacement, which may not be valid (Appleyard and Woolley, 1979).

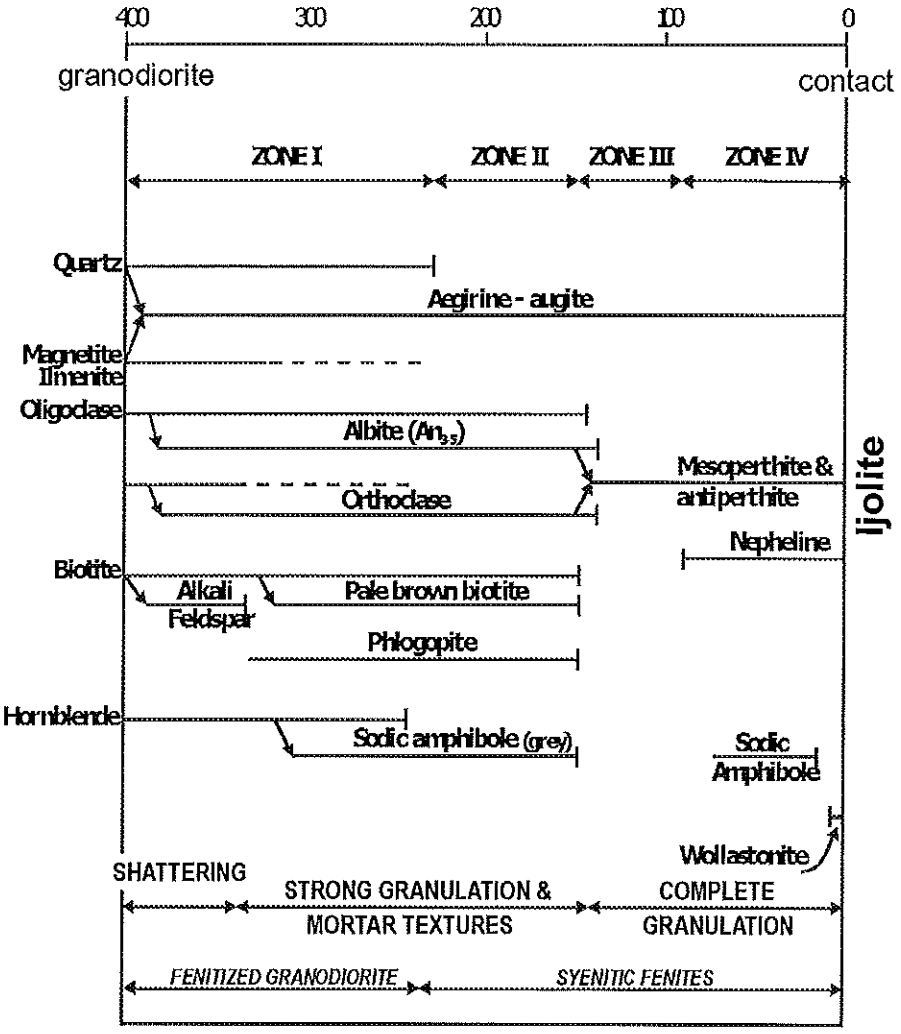

Figure 2: Mineralogical changes during progressive fenitization of granodiorite intruded by ijolite (after Le Bas, 1987).

Appleyard and Woolley (1979) in their study of the Borralan and Sokli fenite suites refined this technique using Gresens' general composition-volume equation (Gresens, 1967), which allows for the quantification of mass-transfer and volume change during fenitization, and showed that modest volume increases accompanied fenitization of these rocks. Work by Kresten (1988) on the fenites from Fen, defined a "chemical index of fenitization" (F.I.) – the sum of mass gains during the process. He suggested its use as a complimentary measure of fenitization. Mass-transfer vs. volume-change relationships have been described using refinements to Gresens' equation. This work, carried out on both aureole and contact fenites, has highlighted the need for distinction to be made between different fenite settings when discussing the chemical and volume changes that take place during metasomatism. A summary of some of the most important work carried

out on addressing the mass-transfer – volume-change problem associated with fenitization is shown in Table 1.

Table 1: Summary of important studies on mass transfer and volume-change during fenitization from various localities

Study	Locality	Volume change during fenitization
Appleyard and Woolley, 1979	Borralan(Scotland), Sokli (Finland)	Modest volume increases
Rubie, 1982	Kisingiri (Western Kenya)	Volume decrease of up to 20% in zones adjacent to intrusion & constant volume beyond this
Kresten, 1988	Fen Complex (Fen, SE Norway)	Slight volume changes throughout aureole
Morogan, 1989	Alnö (Sweden)	General isovolumetric equilibration with modest decrease of volume (6%) in highest grade zones

The characteristics of mass transfer and volume change during the process of fenitization are dependent on a number of variables. Thus, different mass-transfer and volume-change results are observed at different localities. These estimates ultimately provide no resolution as to the exact nature of the fenitizing solutions responsible for what is observed in so many alkali intrusive complexes throughout the world.

Fenitizing Fluids: Nature of the Volatile Phase

Gittins *et al.* (1990) highlighted the uncertainties that exist when attempting to estimate the composition of fluids in equilibrium with carbonatite magmas and further stressed the fact that these compositions are important as they are the fluids that produce fenitization. Most studies on fenites and fenitization focus on the products of this metasomatic process, or otherwise attempt to model the chemical changes observed in natural examples based on a numerical approach, including a number of previously discussed assumptions. Few studies report the compositions of fluid phases that produce fenites, especially those associated with alkali-silicate magmas. Primary fluid and solid inclusions from carbonatites have been used in an attempt to constrain the chemistry of fenitizing solutions. To date these studies have produced no widely applicable results (e.g., Andersen, 1986; Morogan and Lindblom, 1995; Samson *et al.*, 1995). Experimental studies where volatile-rich fluids occur in equilibrium with alkali magmas have been reported by Saha (1961), Gittins *et al.* (1990) and Veksler and Keppler (2000).

Saha (1961) provided the earliest experimental data addressing the problem of fenitizing fluid compositions. He observed fluids enriched in sodium and aluminum in runs with starting compositions Na_2O: Al_2O_3: SiO_2 in the range 1:1:2.5 to 1:1:2.75 (molecular). The synthesized fluids were not analyzed and it was only possible to infer that Na and Al had entered the fluid phase to a much greater extent than silica. McCarthy and Jacobsen (1976) carried out a similar preliminary study on the composition of fenitizing fluids and concluded that the development of feldspar-rich and feldspathoid-bearing assemblages in fenite zones could readily be accounted for by solutions of alkali aluminate. This observation was indicated by both thermodynamic calculations and experimental work, but included no physical measurements or analysis of the composition of the fluid phase.

The limited results above highlight the necessity for further experimental investigation with respect to synthesis and accurate analysis of fenitizing solutions. Recent experimental data presented by Veksler and Keppler (2000), using a double capsule configuration, successfully quantified the fluid-melt partition coefficients in the synthetic system CaO-MgO-Na_2O-CO_2-H_2O. The data presented in their study stressed the important consequences fluid separation and subsequent fluid transport may have on both carbonatite petrogenesis and fenitization.

EXPERIMENTAL METHODS

In their study of the fluids associated with carbonatite magmas, Veksler and Keppler (2000) adopted a double capsule technique to separate the melt and fluid phases in order to overcome quenching problems and hence allow accurate measurement of the high-temperature fluid phase. In their experiments, the double capsule assemblage separates a carbonate powder in a perforated inner capsule from diamond powder and water contained in the outer capsule at the beginning of a run, the rationale being that the carbonatite magma stays in the inner capsule with the aqueous fluid contained in the porous diamond powder in the outer capsule. Thus, the fluid composition can be measured by analyzing the entire contents of the outer capsule, with the exception of C, thereby overcoming the problem of solid phases precipitating from the high-temperature fluid during quenching of the experiment.

In reconnaissance experiments conducted using a similar double capsule approach in this study, small proportions of glass, identical to that in the inner capsule were noted in the outer capsule after quenching. This is perhaps not surprising if it is considered that at equilibrium the fluid is a supercritical solution, saturated with respect to the chemical components of the magma. Thus, magma may be able to form at any point in the fluid, and will be particularly favoured to do so at any point in the outer capsule with a slightly lower temperature. We concluded that small proportions of the magma incorporated into the outer capsule by this mechanism would have made reliable estimation of the composition of the high-temperature fluids impossible. Consequently, we decided to adopt a single capsule approach and rely on accurate separation of the magma component from the fluid-derived products in the quenched experiments by hand picking the glass fragments resulting from magma quenching in the run products under binocular microscope.

The melt and fluid are able to equilibrate completely during the experimental run, and the distribution of the two phases within the capsule is well constrained throughout the experiment. The magma component separated from other run products can then be weighed, and its composition accurately determined in order to calculate the composition of the equilibrium fluid. The mass of aqueous fluid in the capsule during the run can be accurately constrained by difference from the sum of the mass of melt and mass of starting components (oxide powder + deionised water):

mass of starting components = mass of melt + mass of fluid (1)

Following this, the composition of the equilibrium fluid component (with respect to oxide 'X') can be calculated:

%X in starting components × mass of starting components = %X in melt × mass of melt + %X in fluid × mass of fluid (2)

where X = either SiO_2, Al_2O_3, Na_2O or water.

Cold Seal System

Experiments were carried out in cold seal pressure vessels (Fig. 3) at the Experimental Petrology Laboratory at the University of the Witwatersrand. More detailed reviews of this type of equipment are provided by Edgar (1973) and Kerrick (1987). Pressure vessels constructed from René 42® or Inconel® were used. René 42 vessels have an internal diameter (id) of 6.42mm, an outside diameter (od) of 9.60mm and a length of 203mm. Inconel vessels have an id. of 6.27mm, an od. of 14.36mm and a length of 250mm. All vessels are run in a vertical position, using a de-ionised water- pressure medium. Confining pressures are monitored via a HEISE® bourdon tube gauge. Temperature measurement is via a type K thermocouple located in a measuring port machined into the outside of the pressure vessel, directly adjacent to the sample capsule, and a TEMPERATURE CONTROLS® solid state temperature controller with integral ice point. The temperature of the external tube furnace is measured and controlled by an identical device. Temperatures at the sample capsule are readily maintained at ±1°C for the duration of an experiment. The temperature gradient between the inside of the vessel at the hotspot and the thermocouple well was determined using two internal and one external thermocouple, yielding a difference of approximately 1°C. Temperature measurements are believed to be accurate to ± 2°C over the average length (≈ 20mm) of a capsule.

Experiments were carried out at conditions of 850°C and 1kbar. Runs were conducted for periods no shorter than 120 hours, followed by isobaric quenching. Runs using Inconel vessels require <2 minutes to cool from 850°C to 450°C and a further 8 minutes to cool from 450°C to 150°C. Runs using the smaller René 42 vessels cool in approximately half these times. Experiments are conducted either in platinum or gold capsules, sealed by graphite arc welding. The capsules typically have a wall thickness of 0.2mm, a length of 20mm and an internal diameter of 2.93mm.

Starting Materials

The starting materials used in this study were synthesized from high purity powders of aluminum oxide (Al_2O_3), sodium carbonate (Na_2CO_3) and silicon dioxide (SiO_2). These compounds were mixed in desired molar proportions, homogenized using a pestle and mortar and fired at 1000° C, allowing the break-down of $Na_2CO_3. \rightarrow Na_2O$, thus precluding the incorporation of any CO_2 into the starting materials. The resultant glass was ground to a fine powder (approximately 5 μm grain size) in preparation for use in the

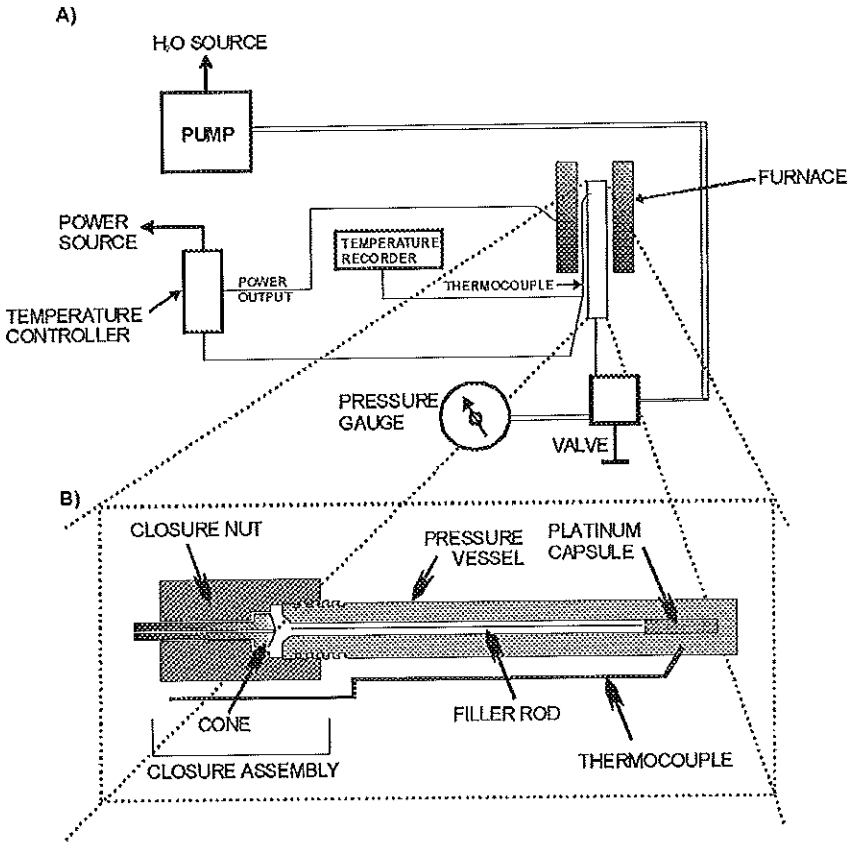

Figure 3: (A) Schematic diagram illustrating the configuration of a conventional cold seal system; and (B) a cross section through a Tuttle-type pressure vessel (Tuttle, 1948,1949), showing the closure assembly and vessel (after Kerrick, 1987).

experiments. Twenty-five starting compositions (Appendix 1) were prepared in this manner. These compositions straddle the nepheline-albite join and include peralkaline and alkaline granitoid compositions (Fig. 4). Starting compositions were loaded into noble metal capsules with 40 wt% deionised water.

Analytical Techniques

The compositions of the glasses were determined using the JEOL SUPERPROBE 733® electron microprobe at the Council for Geoscience, Pretoria. During the glass analyses an accelerating voltage of 15 keV was used, beam current and width were adjusted so as to minimize the problem of loss of sodium through beam excitation. A beam current of 1.9808 $\times 10^{-8}$A and analysis spot size of 20 μm was found to be optimal. Instrument calibration was done using natural mineral standards and checks for Na volatilization were carried out using a comparison of SiO_2, Al_2O_3 and Na_2O in natural glass specimens (National Bureau of Standards): NBS 620, 621 with the published data for these standards. The ZAF correction procedure was employed. The comparative data are presented in Table 2.

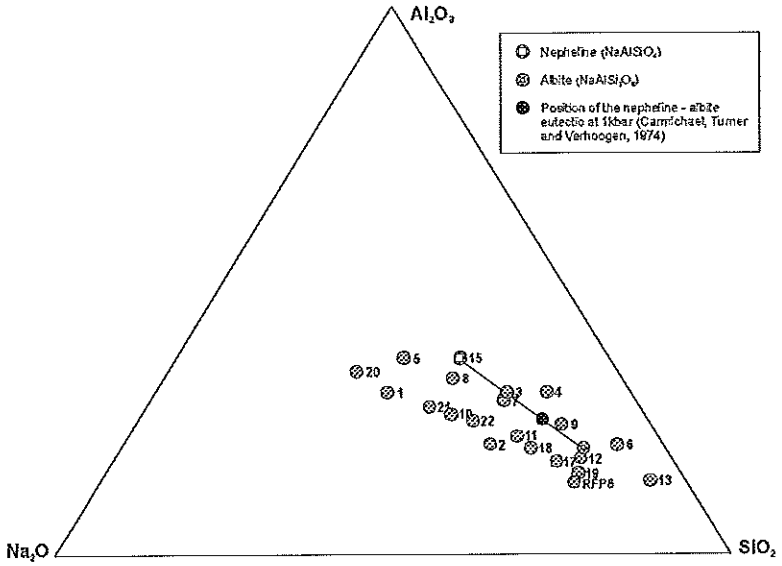

Figure 4: The ternary system Na_2O-Al_2O_3-SiO_2 (wt%), showing the positions of the 21 starting compositions used in this study. The position of the nepheline-albite eutectic at one kilobar (Carmichael et al., 1974), is also shown.

The mineralogy of crystalline glasses was confirmed by EDS analysis, using a NORAN EDS® attached to the JEOL JSM-5600® scanning electron microscope at the Rand Afrikaans University, Johannesburg, with an accelerating voltage of 15kV and a counting time of 100s.

Table 2: Comparison of glass standards for calibration of the JEOL SUPERPROBE 733® used for electron microprobe analysis of quenched melts in this study

	NBS 620		NBS 621	
	Published value	Measured value	Published value	Measured value
Constituent (wt %)				
SiO_2	*72.08*	*72.121*	*71.130*	*71.397*
TiO_2	0.018	0.026	0.014	0.0191
Al_2O_3	*1.800*	*1.924*	*2.760*	*3.007*
Cr_2O_3	-	0.000	-	0.000
FeO	-	0.008	-	0.008
MnO	-	0.000	-	0.035
MgO	3.69	4.062	0.270	0.271
CaO	7.11	7.343	10.710	10.912
Na_2O	*14.39*	*13.934*	*12.740*	*12.607*

Sources of Experimental Error

The major contributions to the error in determining the composition of aqueous equilibrium fluids is attributed to:

(1) incomplete phase separation, i.e. by quench products trapped in the glass, and other fluid derived quench products not extracted during grain picking, which affects the masses of both glass and fluid used in the mass balance calculation. These errors are estimated to be in the range of ± 2 to 5 wt%;

(2) analytical uncertainties in the determination of Na_2O, Al_2O_3 and SiO_2 which accumulate in the H_2O content of the glass which is determined by difference; and

(3) a minor source of error comes from weighing errors in the loading of starting materials into the capsule and is typically in the range of ± 0.005%.

These errors translate into an estimated maximum relative uncertainty of less than ± 3wt% for Na_2O, SiO_2 and Al_2O_3, and ± 10wt% for H_2O in the calculated fluid compositions.

EXPERIMENTAL RESULTS

Twenty-six experiments were carried out. Recovered capsules were weighed, checked for weight loss or gain and carefully opened. Solid and liquid run products were extracted by washing the run products out of the capsule with de-ionised water and careful filtration. The characteristics of each run are summarized in Table 3. The dried, solid run products were separated, by grain picking under a binocular microscope, into the glass derived from the melt and those components derived from the fluid phase during quenching. These were both accurately weighed and stored in a desiccator for future analysis.

Nature of the Solid Products of the Experiments

The product derived from the quenched melt comprises a translucent isotropic glass containing variable proportions of crystals. In most cases the glass had fragmented during opening of the capsule and was present as chunks and shards with obvious concoidal fracture. In at least eight experiments (see Table 3), homogeneous, crystal-free glass was produced (Fig. 5a-c). In most of the experiments the products included either euhedral albite or nepheline crystals as inclusions in the glass (Figs. 5d and 6a-c). Generally, experiments with starting compositions plotting on the peralkaline side of the nepheline-albite join produced homogeneous, crystal-free quenched glasses, while those with starting compositions near the nepheline-albite tie-line, and in the alkaline granitoid field, produced crystal-bearing glasses. Occasionally, the glasses contained bladed, acicular crystals (Fig. 6e). These are interpreted to be quench crystals.

In most of the experiments, a portion of the solid products are interpreted to have formed as quench products from the fluid phase. These occur as radially crystalline beads (Figs.

Table 3: Starting conditions and experimental results. ***Note:*** **All runs were conducted at 850° C and 1 kilobar for periods no shorter than 120 hours**

Run#	Starting composition	Solid:H_2O (molecular)	Initial run charge (g)		Run products
			solid	H_2O	
RFP3	S_1	-	0.12301	-	Glass + fluid quench phase + fluid
RFP6	RFP_6	-	0.12472	0.08998	Glass + fluid quench phase + fluid
RFP9	S_2	0.0363	0.10640	0.07442	Glass + melt quench crystals + fluid quench phase + fluid
RFP10	S_3	0.0309	0.08773	0.07425	Nepheline + glass + fluid
RFP11	S_4	0.0398	0.10508	0.07439	Albite + glass + fluid quench phase + fluid
RFP16	S_6	0.0372	0.08736	0.07649	Glass + melt quench crystals + fluid quench phase + fluid
RFP17	S_5	0.0246	0.07575	0.07387	Nepheline + glass + fluid quench phase + fluid
RFP18	S_7	0.0322	0.09114	0.07379	Nepheline + glass + fluid quench phase + fluid
RFP20	S_8	0.0321	0.08237	0.06498	Nepheline + fluid quench phase + fluid
RFP21	S_1	0.0254	0.04556	0.04230	Glass + fluid quench phase + fluid
RFP22	S_9	0.0179	0.04109	0.04481	Albite + glass + fluid quench phase + fluid
RFP26	S_8	0.0423	0.04160	0.02690	Nepheline + fluid quench phase + fluid
RFP28	S_{10}	0.0278	0.04117	0.03662	Glass + fluid quench phase + fluid
RFP30	S_{12}	0.0281	0.03958	0.03847	Glass + fluid quench phase + fluid
RFP32	S_{11}	0.0288	0.03881	0.03510	Nepheline + glass + fluid quench phase + fluid
RFP33	S_{13}	0.0345	0.04078	0.03404	Quartz + glass + fluid quench phase + fluid
RFP34	S_4	0.0397	0.04140	0.02938	Albite + glass + fluid quench phase + fluid
RFP35	S_{12}	0.0311	0.03987	0.03499	Glass + fluid quench phase + fluid
RFP36	S_{15}	0.0339	0.04028	0.03016	Nepheline + glass + fluid quench phase + fluid
RFP37	S_{17}	0.0347	0.04066	0.02980	Nepheline + glass + fluid quench phase + fluid
RFP38	S_{19}	0.0348	0.03834	0.02982	Nepheline + glass + fluid quench phase + fluid
RFP39	S_{18}	0.0259	0.04134	0.02918	Glass + fluid quench phase + fluid
RFP40	S_2	0.0362	0.04047	0.02838	Glass + fluid quench phase + fluid
RFP41	S_{20}	0.0654	0.03891	0.01418	Nepheline + glass + fluid quench phase + fluid
RFP42	S_{21}	0.0365	0.02973	0.01979	Nepheline + glass + fluid quench phase + fluid
RFP43	S_{22}	0.0377	0.02783	0.01858	Nepheline + glass + fluid quench phase + fluid

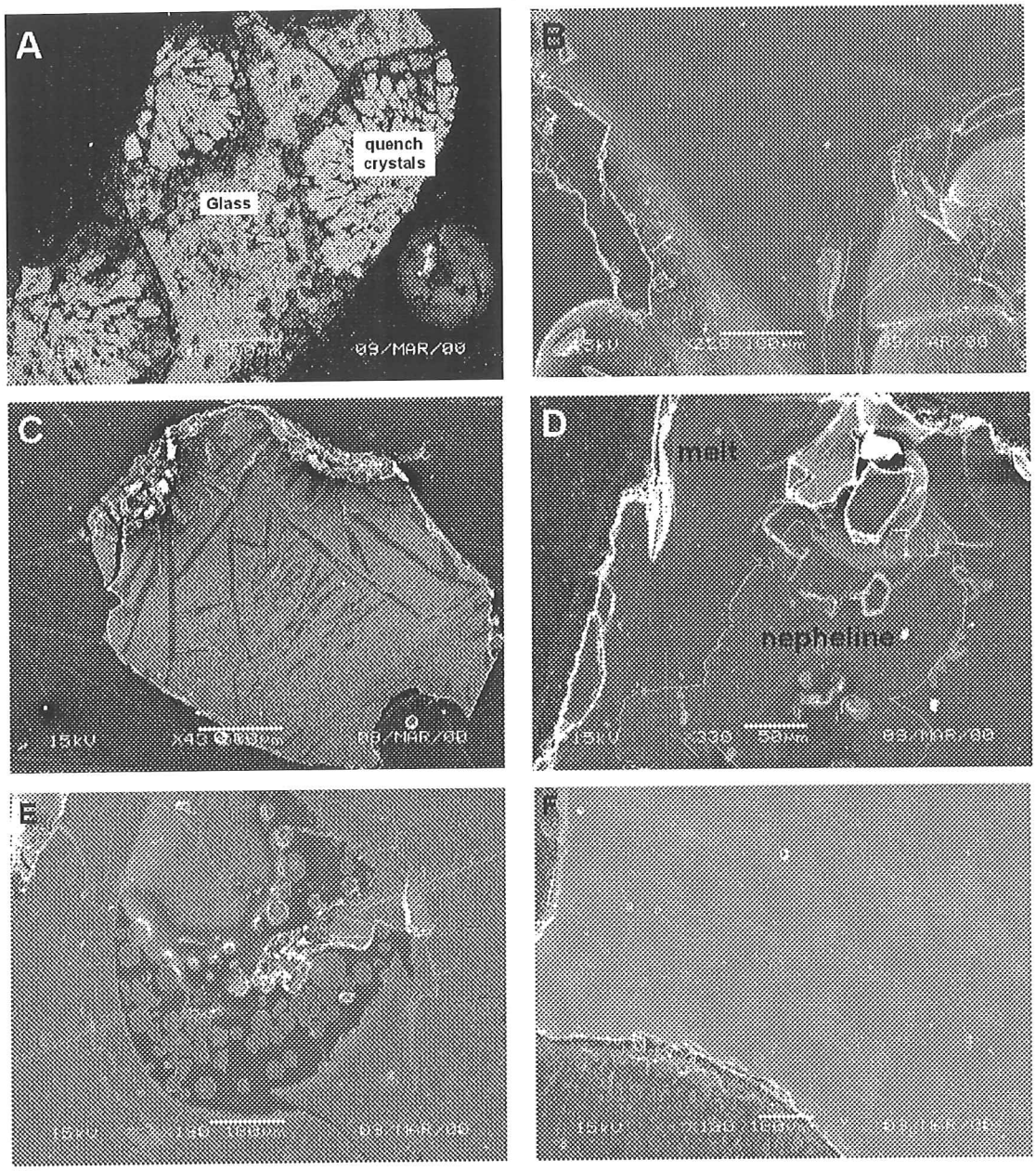

***Figure 5**: Scanning electron microscope images of typical run product textures, all taken in secondary electron mode (except for A taken in back-scattered electron mode):*
(A) glass representing quenched melt and radial crystals derived from the fluid phase during quenching – experiment RFP3; (B) typical occurrence of homogeneous, crystal-free glass from experiment RFP6; (C) uncommon occurrence of acicular quench crystals within the glass – experiment RFP9; (D) nepheline crystals in the glass – experiment RFP27; (E) glass beads with the same composition as the large encircling fragment of glass from experiment RFP35; and (F) homogeneous, crystal-free glass from experiment RFP39, close to the Ne-Ab eutectic.

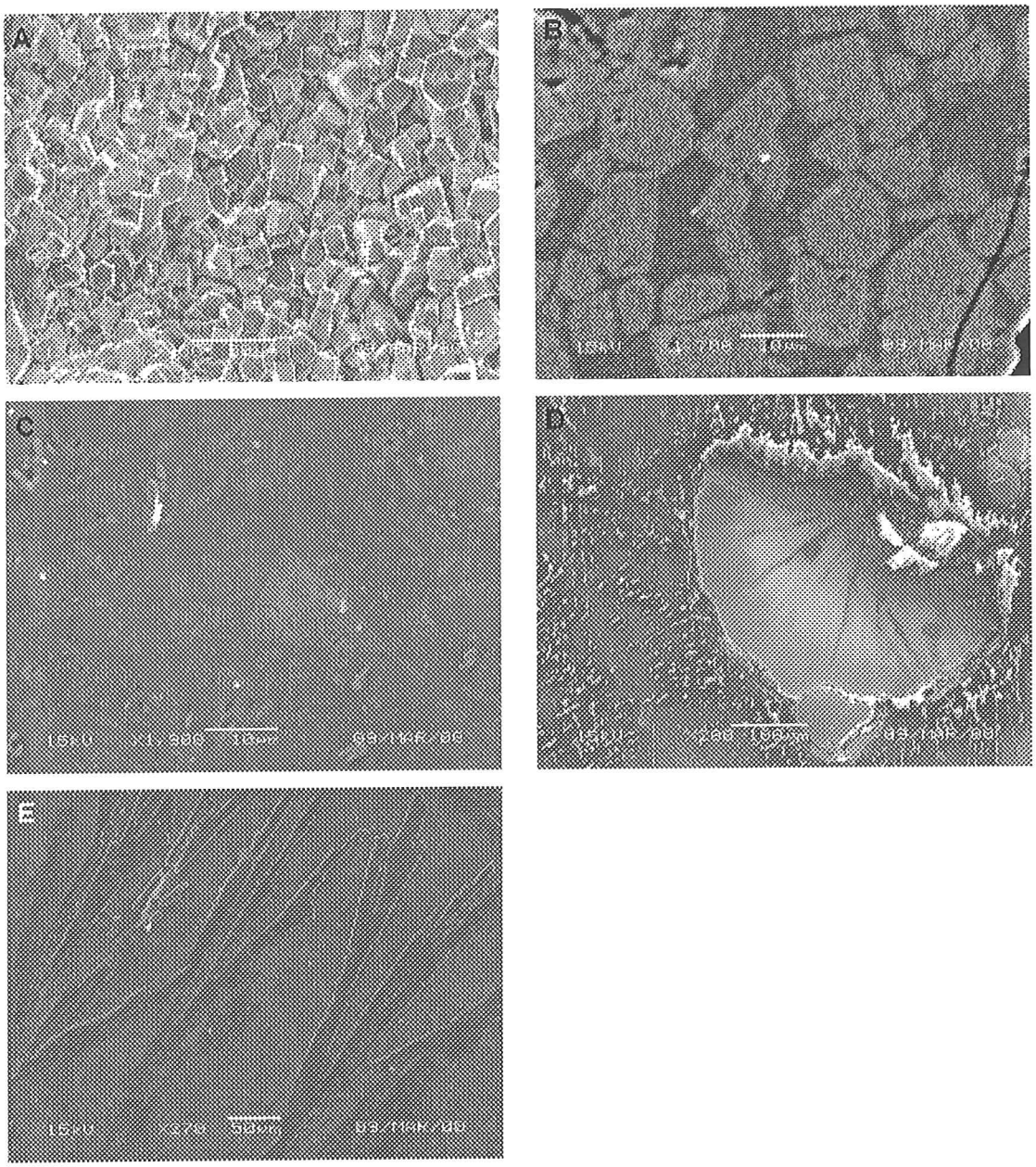

Figure 6: *Scanning electron microscope images (all in secondary electron mode) of equilibrium mineral phases and quench products developed in the run products from experiments RFP 26, 10, 22, 21, 16 and 9, respectively. (A) Hexagonal nepheline crystals exhibiting a cumulus texture in experiment RFP26, with a bulk composition close to that of nepheline; (B) nepheline crystals as inclusions in glass from experiment RFP10; (C) euhedral albite crystals as inclusions in glass from experiment RFP22; (D) a radially crystalline quench bead formed during isobaric quenching of the fluid phase in experiment RFP21; and (E) acicular quench crystals included in glass. This texture is interpreted to form by quench crystallization from the melt during isobaric quenching of experiment RFP9.*

5a and 6d). In some cases these are relatively coarsely crystalline and appear to have formed above the solidus as they produce indentations in the glass (Fig. 5a). In other experiments the radial quench crystals are considerably finer grained, and proportions of the radial textured beads are made up of material that appears amorphous (Fig. 6d).

Composition of the Run Products

Equation 2 can only be applied if no crystalline run products are present. Of the 26 runs only eight were above the liquidus and hence free of crystals. Average melt compositions (determined by EMPA) from these eight experimental runs are presented in Table 4.

Table 4: Average composition of the glasses as determined by EMPA, n = number of analysis points, S = standard deviation

Run #	Starting composition	SiO_2	S	Al_2O_3	S	Na_2O	S	H_2O	S	n
Constituent (wt %)										
RFP3	S_1	35.34	0.73	29.08	1.02	17.78	2.28	17.80	1.76	7
RFP6	RFP_6	67.21	1.22	12.26	0.31	12.73	0.63	7.80	1.35	10
RFP21	S_1	33.91	1.13	30.23	1.37	19.98	2.50	15.88	1.77	9
RFP28	S_{10}	44.57	0.75	23.53	1.00	21.37	2.22	11.55	1.88	12
RFP30	S_{12}	66.60	1.28	17.14	0.51	8.74	1.47	7.51	0.37	18
RFP35	S_{12}	63.60	2.11	16.14	0.65	8.41	1.37	11.85	2.78	20
RFP39	S_{18}	59.67	0.81	22.46	0.51	12.06	0.23	5.72	0.81	30
RFP40	S_2	54.71	0.61	21.88	0.44	13.00	1.65	10.22	1.74	35

Two of the runs were duplicated, one with high silica (S_{12}) and the other with low silica (S_1). Considering the uncertainties in the method discussed earlier, the reproducibility, especially that of water, which is determined by difference, is reasonably good.

The water content of the glasses is relatively high and is compositionally dependent, apparently increasing with decreasing silica content of the melt (Fig. 7), although there is scatter due to the source of error in the method referred to earlier. The dependence of water content on sodium and aluminium cannot be established from the data due to the limited range in Na/Al ratio used in the starting compositions. The glass compositions lie close to the nepheline-albite join (Fig. 8) and some approximate natural alkaline magmas.

DISCUSSION

Composition of Equilibrium Fluids

Fluid compositions, calculated for the data in Table 4 using equation 2, are listed in Table 5, and contain between 40 and 55 wt % dissolved solids and are remarkably concentrated. Fluid compositions could not be calculated for RFP3 and RFP6, because glass and quenched fluid products could not be adequately separated. The proportion of sodium

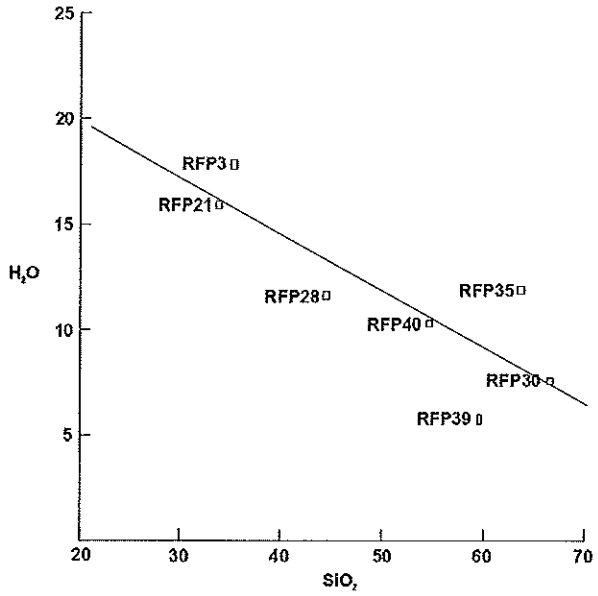

Figure 7: *Binary plot of SiO_2 vs. H_2O (in wt%) for glasses, showing the systematic variation of water content with respect to the amount of SiO_2 in the glass.*

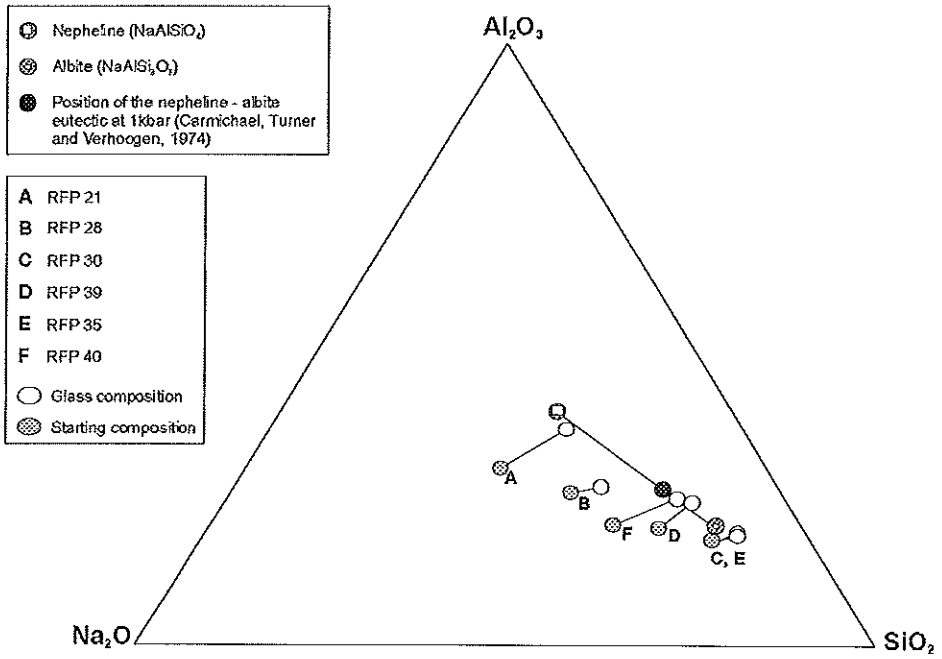

Figure 8: *The ternary system: SiO_2-Al_2O_3-Na_2O + H_2O (in wt%), showing the position of the equilibrium melts with respect to the nepheline-albite join.*

and aluminium in the fluid increases with decreasing silica content in the melt. The replication of these results, as indicated by runs RFP30 and RFP35 is reasonably good.

The calculated fluid compositions and the equilibrium melts are plotted in tetrahedral space; SiO_2 - Al_2O_3 - Na_2O - H_2O (Fig. 9a and 9b). Stereo-tetrahedral plots are shown in Figure 9c and 9d. The equilibrium melt and fluid compositions define two surfaces that appear to be part of a single solvus. With decreasing silica, these surfaces approach one another and suggest that the melt and fluid phases may become miscible at very low silica contents.

Table 5: Calculated equilibrium fluid compositions for glass compositions. All values are in wt%

Run #	Starting composition	SiO_2	Al_2O_3	Na_2O	H_2O
RFP21	S_1	15.75	12.29	27.33	44.84
RFP28	S_{10}	22.84	13.27	18.03	45.20
RFP30	S_{12}	24.97	6.04	8.91	60.38
RFP35	S_{12}	27.91	7.03	9.64	55.69
RFP39	S_{18}	19.46	1.41	16.29	62.84
RFP40	S_2	19.46	5.03	23.85	51.88

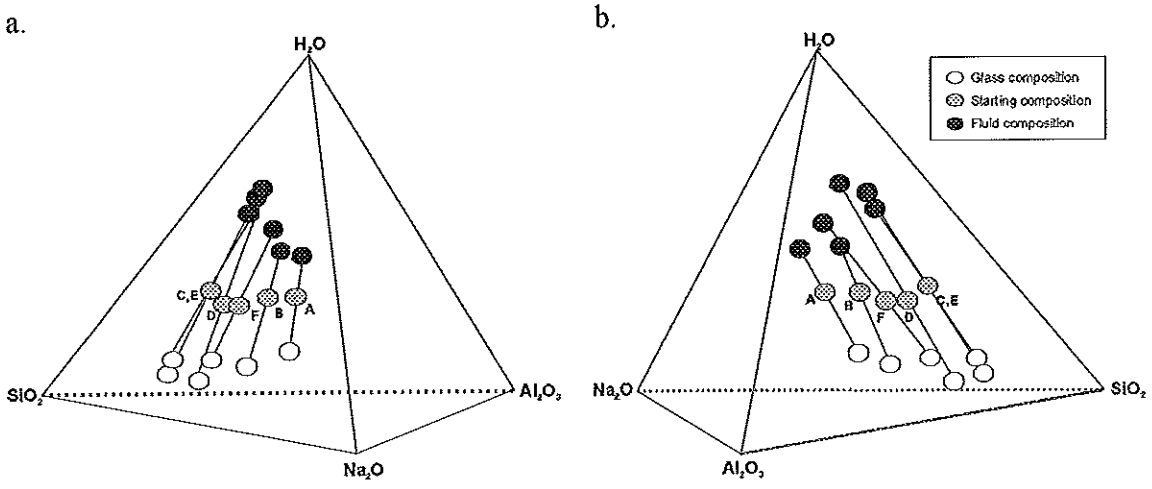

Figure 9: (a, b) Compositions of the starting mixtures, glasses and calculated equilibrium fluids, plotted in the tetrahedral system SiO_2-Al_2O_3-Na_2O-H_2O (wt%). Symbols A-F, as for Figure 8.

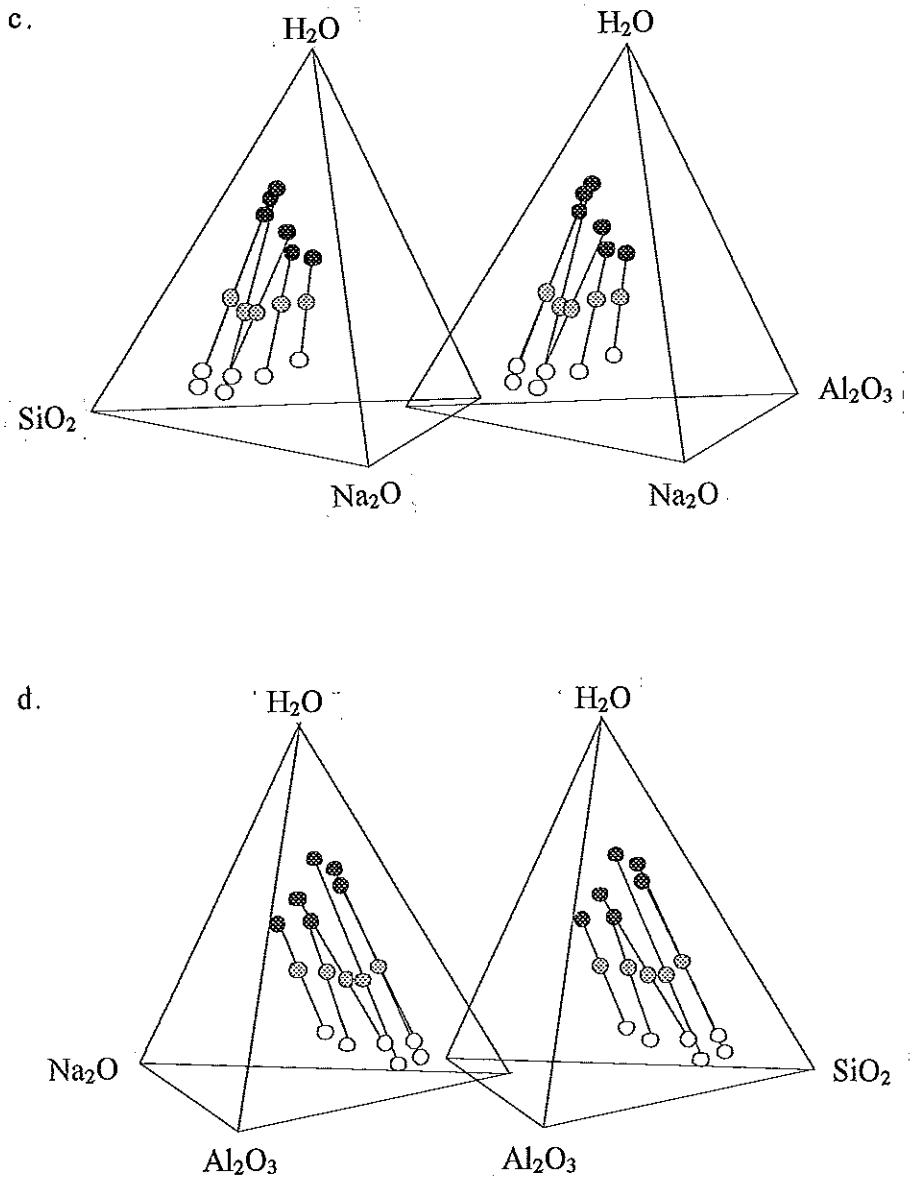

Figure 9: (c, d) stereo-tetrahedral pairs. Symbols as for Figure 9 (a, b).

Modelling the Fenitization Process

The capacity of the fluid compositions calculated in the preceding section to metasomatize granitoid rocks can be evaluated by considering the quantity of fluid required to make a typical granite composition silica undersaturated. This was done by calculating CIPW norms of mixtures of fluid (anhydrous) and a typical granite. The model is simplistic, as the fluid is seen to add its entire composition to the metasomatized product, without dissolving and removing other chemical components. In natural fenites, SiO_2 is believed to be the principal component commonly removed during the metasomatism. The calculations have been performed using granite with the following composition: SiO_2 = 75.34, Al_2O_3 = 11.98, TiO_2 = 0.29, MgO = 0.04, Fe_2O_3 = 3.47, CaO = 1.51, Na_2O = 3.09, K_2O = 4.46 (wt%). Using anhydrous fluid compositions from

experiments RFP21, RFP28 and RFP40, quartz undersaturated assemblages result at relatively low fluid-rock ratios (Fig. 10). In contrast, fluids from RFP35 and RFP39, which have lower Al_2O_3 and Na_2O concentrations, remain quartz saturated to substantially higher fluid-rock ratios (Fig. 10).

Norm calculations involving the granite and fluid composition RFP28 are shown in Table 6. At a very low fluid rock ratio, the metasomatic process manifests itself as a reduction in normative quartz, increase in normative albite, the formation of acmite and the appearance of diopside at the expense of anorthite. At a slightly higher fluid rock ratio, sodium metasilicate appears in the norm and increases in quantity, together with albite while normative quartz decreases. At a fluid rock ratio of approximately 0.8, nepheline appears. This indicates that fluid is converting quartz to albite and excess sodium is reacting with the iron to form acmite and sodium metasilicate.

This sequence is in many ways analogous to what is observed in fenite aureoles in that the early stages of fenitization are charactized by the formation of alkali pyriboles (acmite in the norm), reduction and eventual disappearance of quartz, increase in alkali feldspars, disappearance of anorthite, the appearance of diopsidic pyroxene and the disappearance of hematite (see Fig. 2). The reduction in quartz is most likely due to two processes; one being a conversion to alkali feldspar and the other, the dissolution of quartz. In the sequence of norm calculations (Table 6), the sodium metasilicate component would correspond to the dissolved quartz.

In natural fenites, one of the characteristic features noted is the feldspathization of quartz. This requires the introduction of aluminium in addition to an alkali. The fluids generated experimentally in this work were found to contain significant proportions of aluminium and were hence capable of feldspathization.

Melt compositions, near nepheline on the nepheline-albite join, are in equilibrium with fluids that are capable of converting a granite to a nepheline normative condition (nepheline syenite) at very low fluid rock ratios, whereas compositions towards the albite side of the join require very large fluid rock ratios to accomplish this, or cannot produce nepheline normative compositions at all (Figure 10). This is consistent with field observations. Small alkaline complexes of the ijolite-melteigite series have large metasomatic aureoles in relation to their size, whereas syenitic intrusions do not produce significant metasomatic aureoles.

The model calculations also provide some insight into mass and volume changes that can be expected during fenitization. The change from a granite to nepheline syenite composition in Table 6 involves a small density change (2.75 gm/cm^3 for the granite to 2.72 for the nepheline syenite that develops at a fluid/rock ratio of 0.82, assuming that the sodium metasilicate is removed in solution). The associated mass increase involved (calculated from the decrease in TiO_2 content) is 32%, and the corresponding volume increase is 33%.

Table 6: Normative mineralogies for an average granite (Wits G) and resultant altered compositions

	granite	RFP28 + granite				
Fluid/rock ratio	0.00	0.11	0.33	0.67	0.79	0.82
Constituents (wt%)						
SiO_2	75.34	71.52	69.09	65.57	64.53	64.26
TiO_2	0.29	0.27	0.24	0.21	0.20	0.20
Al_2O_3	11.98	12.35	13.66	15.08	15.50	15.61
FeO	1.75	1.61	1.46	1.27	1.21	1.20
Fe_2O_3	3.47	3.19	2.89	2.51	2.40	2.37
MgO	0.05	0.04	0.04	0.03	0.03	0.03
CaO	1.51	1.39	1.26	1.10	1.05	1.03
Na_2O	3.09	4.99	7.58	10.94	11.94	12.19
K_2O	4.46	4.55	3.71	3.23	3.08	3.05
P_2O_5	0.04	0.04	0.03	0.03	0.03	0.03
MnO	0.10	0.05	0.04	0.04	0.04	0.04
Total	102.02	100.00	100.00	100.00	100.00	100.00
Normative minerals						
Quartz	37.07	24.08	13.45	3.55	0.61	-
Orthoclase	25.81	26.87	21.93	19.06	18.21	18.00
Albite	25.61	38.20	49.57	59.55	62.52	62.89
Anorthite	5.53	-	-	-	-	-
Nepheline	-	-	-	-	-	0.21
Acmite	-	3.55	8.37	7.27	6.95	6.86
Na-metasilicate	-	-	1.18	5.76	7.12	7.47
Diopside	-	5.81	5.34	4.64	4.44	4.38
Hypersthene	0.10	-	-	-	-	-
Magnetite	4.87	2.84	-	-	-	-
Hematite	0.05	-	-	-	-	-
Ilmenite	0.54	0.51	0.46	0.40	0.38	0.38
Apatite	0.09	0.09	0.07	0.06	0.06	0.06

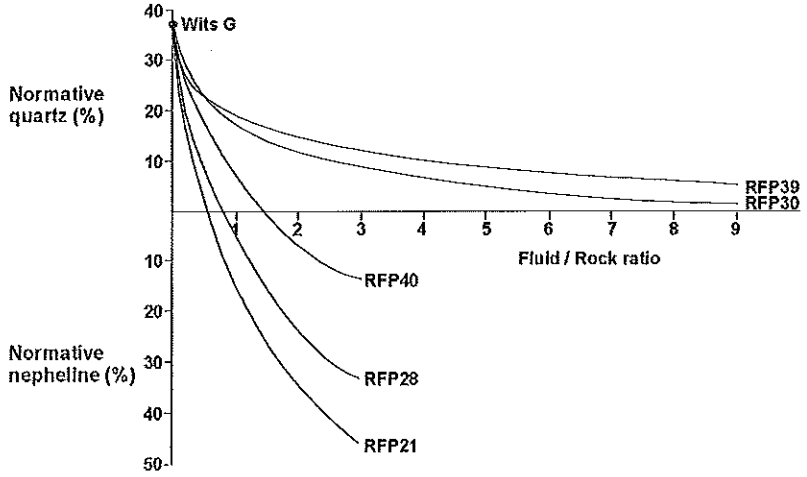

Figure 10: An illustration of the fenitization potential of the four calculated fluid compositions when reacted with the Wits G granitoid composition. Normative mineralogies for the resultant, altered compositions are shown together with respective fluid-rock ratios.

This model indicates that the fluids produced experimentally are capable of inducing nepheline normative compositions at small fluid/rock ratios and that there is a significant volume increase, which could be responsible for the granulation textures commonly observed in fenite aureoles.

CONCLUSIONS

Melt compositions that plot on, or close to the nephleline-albite join can dissolve substantial quantities of water, which increases with decreasing SiO_2 content. These melts are in equilibrium with fluids that contain very large proportions of dissolved solids (SiO_2, Al_2O_3 and Na_2O), in the range 40 – 55 wt%. Fluids in equilibrium with melts that plot towards the nepheline-rich side of the nepheline-albite join are capable of converting a granite to a nepheline normative composition at fluid/rock ratios less than one. The model calculations of this rock reaction show that these fluids produce a paragenetic sequence of alteration very similar to those observed in fenite aureoles (e.g. Le Bas, 1987). Moreover, these fluids are capable of both albitizing and dissolving quartz, due to their high Na and Al contents. Model calculations indicate that reaction of these fluids with a granite is associated with significant volume increase, which may account for the granulation observed in fenite aureoles.

Experiments carried out in this work were limited in scope and confined to the system Na_2O-Al_2O_3-SiO_2-H_2O at conditions of 1 kilobar and 850°C. Fluid and melt compositions generated in this study appear to define a single solvus surface. Only a very limited region of this solvus has been explored and will undoubtedly change with changing P and T, and considerable more experimental work will be needed to fully define both the surface and its P-T dependence. Nevertheless, we believe that this work has revealed the geologically most relevant portion of the solvus at appropriate P and T, and that significant new insight into the nature of fenitization has been attained.

ACKNOWLEDGEMENTS

The authors wish to thank Dr. D. de Bruin and Mrs. A. Walliser of the Council for Geoscience, Pretoria for their assistance during electron microprobe analysis of quenched glasses. The authors also wish to thank Rand Afrikaans University their assistance with SEM analysis. Research funding by the National Research Foundation is gratefully acknowledged.

REFERENCES

Andersen, T., 1986. Magmatic fluids in the Fen carbonatite complex, S.E. Norway: evidence of mid-crustal fractionation from solid and fluid inclusions in apatite. *Contributions to Mineralogy and Petrology*, **93**, 491-503.

Andersen, T. and Qvale, H., 1986. Pyroclastic mechanisms for carbonatite intrusion: evidence from intrusives in the Fen central complex, SE Norway. *Journal of Geology*, **94**, 762-769.

Appleyard, E.C and Woolley, A.R., 1979. Fenitization: an example of the problems characterizing mass transfer and volume changes. *Chemical Geology*, **26**, 1-15.

Brögger, W.C., (1921). Die Eruptivgesteine des Kristianiagebeites, IV., Das Fengebeit in Telemark. *Selsk. Vidensk. Selsk. Skrifter.* I, *Math. Naturv. Kl.*, (1920), **9**, 1-408.

Carmichael, I.S.E., Turner, F.J. and Verhoogen, J., 1974. *Igneous Petrology.* International Series in Earth and Planetary Sciences, McGraw-Hill, New York, 739pp.

Cooper, A. F., 1971. Carbonatites and fenitization associated with a lamprophyric dike-swarm intrusive into schists of the New Zealand geosyncline. *Bulletin of the Geological Society of America,* **82**, 1327-1340.

Currie, K.L., 1971. A study of potash fenitization around the Brent crater, Ontario : a Paleozoic alkaline complex. *Canadian Journal of Earth Sciences*, **8**, 481-517.

Currie, K.L. and Ferguson, J., 1971. A study of fenitization around the alkaline carbonatite complex at Callander Bay, Ontario. *Canadian Journal of Earth Sciences*, **8**, 498-517.

Currie, K.L. and Ferguson, J., 1972. A study of fenitization in mafic rocks, with special reference to the Callander Bay Complex. *Canadian Journal of Earth Sciences*, **9**, 1254-1261.

Currie, K.L., Knutson, J. and Temby, P.A., 1992. The Mud Tank carbonatite complex, central Australia – an example of metasomatism at mid-crustal levels. *Contributions to Mineralogy and Petrology*, **109**, 326-339.

Dawson, J.B. and Smith, J.V., 1992. Potassium loss during metasomatic alteration of mica pyroxenite from Oldoinyo Lengai, northern Tanzania: contrasts with fenitization. *Contributions to Mineralogy and Petrology*, **112**, 254-260.

Edgar, A.D., 1973. *Experimental Petrology: Basic Principles and Techniques.* Oxford University Press, 217 pp.

Garson, M. S., Coats, J.S., Rock, N.M.S. and Deans, T., 1984. Fenites, breccia dykes, albitites, and carbonatitic veins near the Great Glen Fault, Inverness, Scotland. *Journal of the Geological Society, London,* **141**, 711-732.

Gittins, J., 1989. The origin and evolution of carbonatite magmas. *In:* Bell, K. (ed.), *Carbonatites : Genesis and Evolution.* Unwin Hyman, London, 618pp.

Gittins, J., Beckett, M. F. and Jago, B. C., 1990. Composition of the fluid phase accompanying carbonatite magma: A critical examination. *American Mineralogist*, **75**, 1106-1109.

Gresens, R.L., 1967. Composition - volume relationships in metasomatism. *Chemical Geology*, **2**, 47-65.

Heinrich, E. Wm., 1966. *The Geology of Carbonatites.* Rand McNally, Chicago, 555pp.

Kerrick, D.M., 1987. Cold-seal systems. *In:* Ulmer, G. C. and Barnes, H.L. (eds.), *Hydrothermal Experimental Techniques.* John Wiley & Sons, New York, 523 pp.

Kresten, P., 1988. The chemistry of fenitization: examples from Fen, Norway. *Chemical Geology*, **68**, 329-349.

Kresten, P. and Morogan, V., 1986. Fenitization at the Fen Complex, southern Norway. *Lithos*, **19**, 27-42.

Le Bas, M.J., 1987. Nephelinites and carbonatites. *In*: Fitton, J.G. and Upton, B.G.J. (eds.), *Alkaline Igneous Rocks.* Geological Society Special Publication No. **30**, pp. 53-83.

McCarthy, T.S. and Jacobsen, J.B.E., 1976. The composition of fenitizing fluids. *University of the Witwatersrand, Johannesburg* (unpubl.), 11pp.

McKie, D., 1966. Fenitization, 261-294. *In*: Tuttle, O.F. and Gittins, J. (eds.) *Carbonatites,* Interscience, New York, 591 pp.

Morogan, V., 1984. Ijolite versus carbonatite as sources of fenitization. *Terra Nova*, **6**(2), 166-176.

Morogan, V., 1989. Mass transfer and REE mobility during fenitization at Alnö, Sweden. *Contributions to Mineralogy and Petrology*, **103**, 25-34.

Morogan, V. and Lindblom, S., 1995. Volatiles associated with the alkaline-carbonatite magmatism at Alnö, Sweden: a study of fluid and solid inclusions in minerals from the Langarsholmen ring complex. *Contributions to Mineralogy and Petrology*, **122**, 262-274.

Morogan, V. and Woolley, A.R., 1988. Fenitization at the Alnö carbonatite complex, Sweden; distribution, mineralogy and genesis. *Contributions to Mineralogy and Petrology,* **100**, 169-182.

Pearson, J. M. and Taylor, W.R., 1996. Mineralogy and geochemistry of fenitized alkaline ultrabasic sills of the Gifford Creek Complex, Gascoyne Province, Western Australia. *Canadian Mineralogist*, **34**, 201-219.

Robins, B., 1984. Petrography and petrogenesis of nephelinized gabbros from Finnmark, Northern Norway. *Contributions to Mineralogy and Petrology*, **86**, 170-177.

Robins, B. and Tysseland, M., (1983). The geology, geochemistry and origin of ultrabasic fenites associated with the pollen carbonatite (Finnmark, Norway). Chemical Geology, **40**, 65-95.

Rubie, D.C., 1982. Mass transfer and volume change during alkali metasomatism at Kisingiri, Western Kenya. *Lithos*, **15**, 99-109.

Rubie, D.C. and Gunter, W.D., 1983. The role of speciation in alkaline igneous fluids during fenite metasomatism. *Contributions to Mineralogy and Petrology*, **82**, 165-175.

Saha, P., 1961. The system nepheline-albite-H_2O. *American Mineralogist*, **46**, p. 859.

Saether, E., 1957. The alkaline rock province of the Fen area in southern Norway. *K. Nor. Vidensk. Selsk. Skr.*, **1**, 148pp.

Samson, I.N., Williams-Jones, A.E. and Liu, W., 1995. The chemistry of hydrothermal fluids in carbonatites: evidence from leachate and SEM-decrepitate analysis of fluid inclusions from Oka, Quebec, Canada. *Geochimica et Cosmochimica Acta*, **59**, 1979-1989.

Siemiatkowska, K.M. and Martin, R.F., 1975. Fenitization of Mississagi quartzite, Sudbury area, Ontario. *Bulletin of the Geological Society of America*, **86**, 1109-1122.

Strauss, C.A. and Truter, F.A., 1950. The alkali complex at Spitzkop, Sekukuniland, Eastern Transvaal. *Transactions of the Geological Society of South Africa*, **53**, 81-125.

Vartiainen, H. and Woolley, A.R., 1976. The petrography, mineralogy and chemistry of the fenites of the Sokli carbonatite intrusion, Finland. *Bulletin of the Geological Survey of Finland*, No. **280**, 87pp.

Veksler, I.V. and Keppler, H., 2000. Partitioning of Mg, Ca and Na between carbonatite melt and hydrous fluid at 0.1-0.2 GPa. *Contributions to Mineralogy and Petrology*, **138**, 27-34.

Verwoerd, W.J., 1966. South African carbonatites and their probable mode of origin. *Annals of the University of Stellenbosch, Series A*, **41** (2), 113-233.

Von Eckermann, H., 1948. The alkaline district of Alnö Island. *Sveriges Geol. Unders. Ca.*, **36**, 1-176.

oOo

APPENDIX

Appendix 1. Oxide compositions of twenty-five starting compositions used in this study

Starting Comp.	SiO_2	Al_2O_3	Na_2O
Constituent oxides (wt%)			
S_1	34.71	29.46	35.82
RFP_6	70.58	13.10	16.32
S_2	54.59	20.07	25.34
S_3	52.37	29.62	18.01
S_4	58.30	29.67	12.03
S_6	73.44	20.08	6.48
S_5	33.76	35.79	30.46
S_7	52.71	28.17	19.12
S_8	43.06	32.18	24.76
S_9	63.38	23.65	12.98
S_{10}	46.12	25.43	28.45
S_{11}	57.94	21.52	20.54
S_{12}	69.29	17.56	13.15
S_{13}	81.53	13.60	4.86
S_{15}	42.30	35.89	21.82
S_{17}	65.91	17.09	17.00
S_{18}	58.98	19.51	19.51
S_{19}	70.26	14.92	14.82
S_{20}	28.21	33.39	38.40
S_{21}	42.25	26.89	30.86
S_{22}	49.99	24.24	25.78